IOPscience

This site uses cookies. By continuing to use this site you agree to our use of cookies. To find out more, see our Privacy and Cookies policy.





A NOTICE: Ensuring subscriber access to content on IOPscience throughout the coronavirus outbreak - see our remote access guidelines.

A Comparison of the Well-constrained Geometry of V444 Cygni and Two Possible Analogs: WR 21 and WR 62a

Rachel A. Johnson¹ D, Andrew G. Fullard¹ D, Jamie R. Lomax² D, Kevin Cooper¹, Daniela Leon-Alvarez¹,

Jennifer L. Hoffman¹ , and Kenneth H. Nordsieck³

Published 2019 October 4 • © 2019. The American Astronomical Society. All rights reserved.

Research Notes of the AAS, Volume 3, Number 10

rachel.johnson387@du.edu

Rachel A. Johnson (D) https://orcid.org/0000-0001-5022-0472

Andrew G. Fullard https://orcid.org/0000-0001-7343-1678

Jamie R. Lomax https://orcid.org/0000-0001-8470-0853

1 of 7 6/27/2020, 3:09 PM

¹ University of Denver, USA

² United States Naval Academy, USA

³ University of Wisconsin-Madison, USA

Jennifer L. Hoffman (D) https://orcid.org/0000-0003-1495-2275

Received 2019 October 1

Accepted 2019 October 2

Published 2019 October 4

Rachel A. Johnson et al 2019 Res. Notes AAS 3 146

https://doi.org/10.3847/2515-5172/ab4a12

Wolf-Rayet stars; Close binary stars; Massive stars; Spectropolarimetry

Export citation and abstract

BibTeX

RIS

1. Introduction

Massive stars show a statistical propensity for forming in binary systems, where the presence of a companion affects their evolution (Sana et al. 2012). WR+O binary systems are particularly interesting examples, as they may create the rapidly rotating WR stars that likely give rise to ultra-energetic GRB explosions (Woosley et al. 1993; Shara et al. 2017).

V444 Cygni is a well-studied eclipsing WN5+O6II-V system (i = 78, 4.2 days period; Eriş & Ekmekçi 2011) whose polarimetric behavior is influenced by a rotationally distorted cavity in the WN star wind (St-Louis et al. 1993; Lomax et al. 2015). In this paper, we compare the line polarization behavior of V444 Cyg, including 10 new observations, with that of two similar but non-eclipsing WR+O binaries: WR 21 (WN5+O7; $i = 50^{\circ}-69^{\circ}$; 8.9 days period; Lamontagne et al. 1996; Fahed & Moffat 2012) and WR 62a (WN5+O5.5-6, i unknown; 9.1 days period; Shara et al. 1999; Collado et al. 2013). We aim to assess whether the latter 2 systems show similar wind structures to that of V444 Cyg.

2. Observations

We obtained new polarization spectra for V444 Cyg between 2013 July and October using the Half-Wave

Spectropolarimeter (HPOL) on the University of Toledo's 1 m Ritter Observatory telescope (Davidson et al. 2014). We calculated orbital phases for all V444 Cyg observations, including those in Lomax et al. (2015), using the updated quadratic ephemeris of Eriş & Ekmekçi (2011).

The spectropolarimetric data for WR 21 and WR 62a were collected between 2017 December and 2019 August with the Robert Stobie Spectrograph (RSS; Kobulnicky et al. 2003) on the 11 m Southern African Large Telescope (SALT; Buckley et al. 2006). We used ephemerides from Fahed & Moffat (2012, WR 21) and Collado et al. (2013, WR 62a) to determine the phases of these observations.

3. Line Polarization

For each target, we obtained the integrated polarization in the He II $\lambda 4686$ line using the *pfew* method (Lomax et al. 2015). To account for the different orientations of the three objects, we rotated the line polarization data for each to the mean position angle of its nearby continuum; this relates the polarization of each line to the intrinsic axis of its system. We did not attempt to remove interstellar polarization. We compare the results in Figure 1.

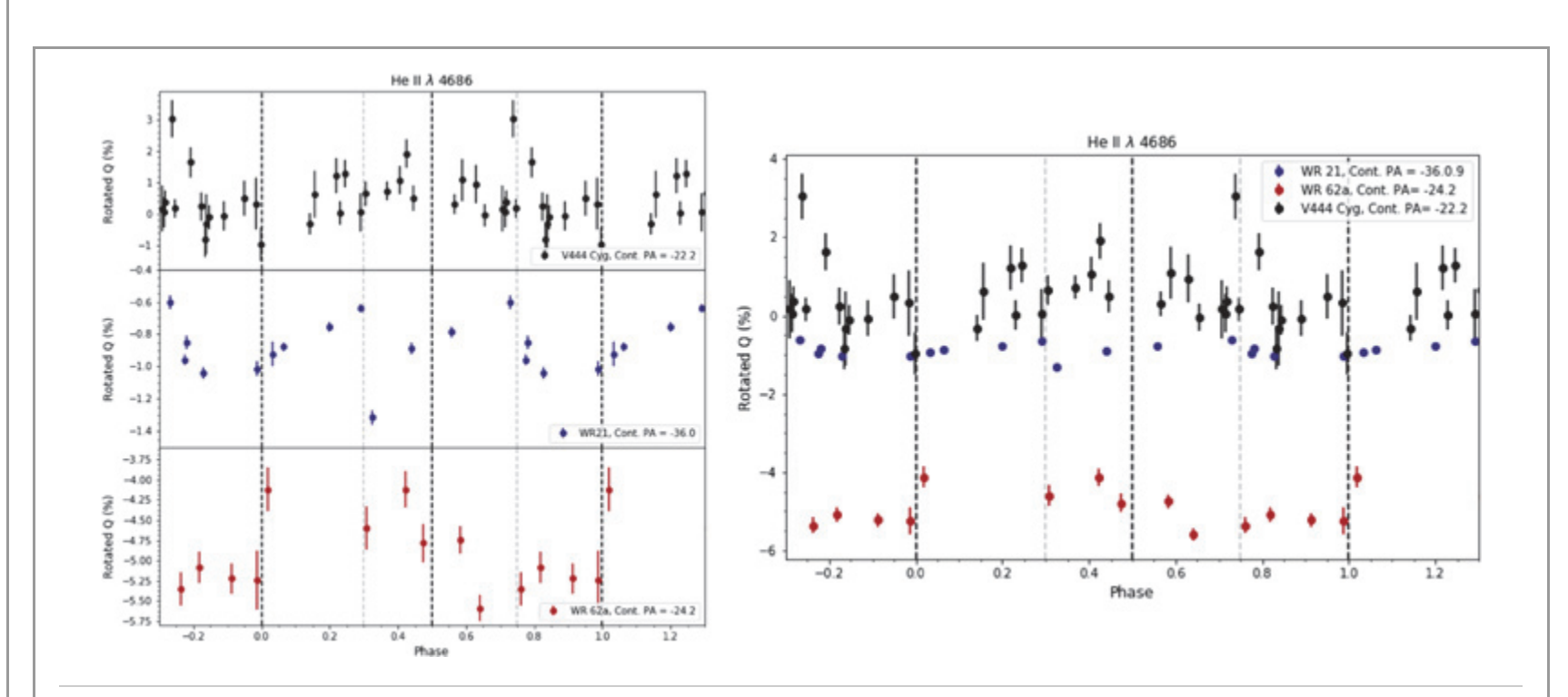


Figure 1. Rotated integrated He II λ 4686 polarization as a function of orbital phase for our three targets. Error bars represent 1 σ intrinsic uncertainties. Black dashed lines mark eclipse phases; gray dashed lines indicate shock cone boundaries determined from an X-ray model of V4444 Cyg (Lomax et al. 2015). Differences in absolute q values are likely due to differing interstellar polarization contributions.

4. Discussion

The new data for V444 Cyg support our previous conclusions that the line polarization behavior reflects the influence of a shock cone in the colliding winds between phases 0.3 and 0.75 (Lomax et al. 2015). The differences among the three curves arise from a combination of factors: the orbital period determines the amount of Coriolis distortion of the shock cone (Lomax et al. 2015); the orbital separation controls the amount of radiative braking/inhibition and thus the

opening angle of the cone (Stevens & Pollock 1994; Owocki & Gayley 1995); and the orbital inclination determines the resulting asphericity of the wind seen from our viewing angle. WR 21 shows similar polarization variations to V444 Cyg at similar phases, but with a smaller amplitude, suggesting it may have a similar wind geometry but a lower inclination angle. WR 62a shows intrinsic variations that do not resemble the others', which may indicate that its inclination is very low. Further analysis and modeling of the line variations will allow quantitative comparisons of the inclination angles and other system properties.

We thank A. Moffat and N. St-Louis for collaborative discussions, N. Richardson for collecting the V444 Cyg data, and the SALT observing team for collecting the southern WR data. This research is supported by NSF awards AST-1816944 and AST-1841578 and uses data from the SALT observing program 2018-2-MLT-005.

— Hide references

- ↑ Buckley D. A. H., Swart G. P. and Meiring J. G. 2006 *Proc. SPIE* **6267** 62670Z Crossref ADS Google Scholar
- ↑ Collado A., Gamen R. and Barbá R. H. 2013 *A&A* **552** A22 Crossref ADS Google Scholar
- ↑ Davidson J. W., Bjorkman K. S., Hoffman J. L. *et al* 2014 *JAI* **3** 1450009 ADS Google Scholar
- <u>†</u> Eriş F. and Ekmekçi F. 2011 *AN* **332** 616 ADS Google Scholar
- ↑ Fahed R. and Moffat A. 2012 MNRAS 424 1601 Crossref ADS Google Scholar

- ↑ Kobulnicky H. A., Nordsieck K. H., Burgh E. B. *et al* 2003 *Proc. SPIE* **4841** 1634 Crossref ADS Google Scholar
- ↑ Lamontagne R., Moffat A. F. J., Drissen L., Robert C. and Matthews J. M. 1996 AJ 112 2227
 Crossref ADS Google Scholar
- ↑ Lomax J. R., Nazé Y., Hoffman J. L. *et al* 2015 *A&A* **573** A43 Crossref ADS Google Scholar
- ↑ Owocki S. P. and Gayley K. G. 1995 *ApJL* **454** L145
 IOPscience (https://iopscience.iop.org/1538-4357/454/2/L145)
 ADS Google Scholar
- ↑ Sana H., de Mink S. E., de Koter A. *et al* 2012 *Sci* **337** 444 Crossref ADS Google Scholar
- ↑ Shara M. M., Crawford S. M., Vanbeveren D. *et al* 2017 *MNRAS* **464** 2066 Crossref ADS Google Scholar
- ↑ Shara M. M., Moffat A. F. J., Smith L. F. *et al* 1999 *AJ* **118** 390 IOPscience (https://iopscience.iop.org/1538-3881/118/1/390) ADS Google Scholar
- ↑ Stevens I. R. and Pollock A. M. T. 1994 *MNRAS* **269** 226 Crossref ADS Google Scholar
- ↑ St-Louis N., Moffat A., Lapointe L. *et al* 1993 *ApJ* **410** 342 Crossref ADS Google Scholar
- ↑ Woosley S. E., Langer N. and Weaver T. A. 1993 *ApJ* **411** 823 Crossref ADS Google Scholar

 $6 ext{ of } 7$ $6/27/2020, 3:09 ext{ PM}$

Export references:

BibTeX

RIS

7 of 7 6/27/2020, 3:09 PM